Ultrafast Magnetization of a Dense Molecular Gas with an Optical Centrifuge

A. A. Milner, A. Korobenko, and V. Milner
Department of Physics & Astronomy, The University of British Columbia, V6T 1Z1 Vancouver, Canada
(Received 26 December 2016; published 16 June 2017)

Strong laser-induced magnetization of oxygen gas at room temperature and atmospheric pressure is achieved experimentally on the subnanosecond time scale. The method is based on controlling the electronic spin of paramagnetic molecules by means of manipulating their rotation with an optical centrifuge. Spin-rotational coupling results in a high degree of spin polarization on the order of one Bohr magneton per centrifuged molecule. Owing to the nonresonant interaction with the laser pulses, the demonstrated technique is applicable to a broad class of paramagnetic rotors. Executed in a high-density gas, it may offer an efficient way of generating macroscopic magnetic fields remotely (as shown in this work) and producing a large amount of spin-polarized electrons.

DOI: 10.1103/PhysRevLett.118.243201

Numerous studies in fundamental and applied sciences utilize gases with spin-polarized electrons. Such gases are used for converting their electronic polarization to the polarization of nuclear spins [1], one of the key elements in nuclear magnetic resonance (NMR) imaging [2], and providing a source of spin-polarized electrons [3,4] for particle-physics experiments [5], as well as for probing molecular dynamics during chemical reactions and analyzing the electronic properties of materials [6].

At room temperature, lining up electronic spins by applying even the strongest laboratory-scale magnetic field is inefficient. In a widely used alternative approach, spin alignment is executed by means of optical pumping, in which an atom undergoes repetitive cycles of the resonant absorption of circularly polarized light, followed by spontaneous emission [7]. Spontaneous life time dictates the time scale on the order of 100 ns for achieving a high degree of spin polarization. The process can be executed faster if the polarized electron is ejected from the parent atom by means of either frequency-resolved [8,9] or time-resolved [10,11] multiphoton ionization.

Methods that rely on a resonant atom-laser interaction are limited by the availability of strong light sources with the required wavelength. Alkali vapors—the most common gases for which such sources are readily available—have to be kept at low densities on the order of 10^{14} cm^{-3} to prevent clusterization, strong absorption of pumping light and collisional depolarization [12,13], thus providing a relatively low amount of spin polarized electrons. High densities of rare gases, on the other hand, cannot be fully exploited because of the lack of high-intensity tunable vacuum ultraviolet sources.

In this Letter, we demonstrate an alternative method of electronic spin polarization. The technique is based on the unidirectional rotation of molecules in an optical centrifuge [14,15]. Unlike optical pumping, it operates far off electronic resonances and is applicable to a broad class of Hund's case (b) molecules. Owing to its nonresonant nature, the process can be carried out in a dense gas—here, in oxygen at atmospheric pressure. Even though only a few percent of O_2 molecules are centrifuged at room temperature, the observed density of polarized electrons exceeds 6×10^{17} cm^{-3}. Such high degree of gas magnetization, 3 orders of magnitude above the magnetization typically obtained with optical pumping, corresponds to the centrifuge-induced magnetic field on the scale of tens of milligauss, detectable with a simple pickup coil. Finally, we show that the electronic polarization occurs on a subnanosecond time scale and can be enhanced, as well as accelerated, by placing the gas in a permanent external magnetic field.

Our optical setup has been described elsewhere [16]. Briefly, the output beam of a broadband Ti:Sapphire laser (30 fs, 10 mJ at 800 nm) passes through a centrifuge pulse shaper, where the pulses are split into two spectral components, whose frequencies are linearly chirped in time. The applied chirps are equal in magnitude ($\approx$0.17 THz/ps), but opposite in sign. The two spectral components are separately amplified to $\approx$15 mJ each in a home-built multipass amplifier, circularly polarized in opposite directions and combined in space and time to produce the field of an optical centrifuge, illustrated in Fig. 1.

Centrifuge pulses were focused with a $f = 1000$ mm lens inside a hermetic chamber, filled with oxygen at room temperature and variable pressure. To determine the degree of rotational excitation, we used coherent Raman spectroscopy. The latter is executed by sending a weak narrow-band probe pulse through the gas of centrifuged O_2 molecules and measuring the rotational Raman shift [17,18]. Our centrifuge shaper enables precise control of the molecular angular momentum, which in this work was varied between $N = 25$ and $N = 89$.

The magnetization of oxygen gas was detected with a pick-up coil, centered at the location of the centrifuged volume [Fig. 1(a)]. The coil was connected to a 3 GHz bandwidth oscilloscope, which recorded the time-dependent electromotive force EMF $\mathcal{E}(t)$. The latter is proportional to

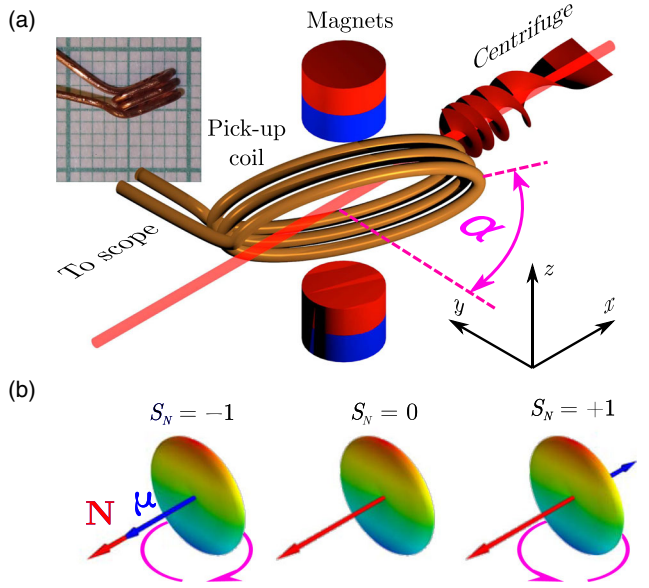

FIG. 1. (a) Experimental configuration. Centrifuge pulses, illustrated with a corkscrew-shaped red surface, pass through a pick-up coil between a pair of permanent magnets. The coil, pictured in the inset, was tilted by an angle $\alpha = 59°$, had an elliptical cross section of 0.93×3.8 mm^2, 2.5 turns, and was used for measuring the transverse magnetization (see text). Another coil (not shown) with a circular cross section of 1.2 mm diameter, 4.5 turns, and its axis collinear with the centrifuge beam (thick red line) was used for detecting the longitudinal magnetization. (b) Molecular gyroscopes, represented by the disk-shaped distributions of molecular axes in the plane of rotation, with three possible projections of the electronic spin $\boldsymbol{\mu}$ (short blue arrows) on the molecular angular momentum $\mathbf{N}$ (long red arrows). Pink arrows under the left and right gyroscope show the direction of Larmor precession in the external magnetic field (see text).

the time derivative of the induced magnetization $\mathbf{M}$ perpendicular to the plane of the coil. Hereafter, we refer to the projections of $\mathbf{M}$ on the laser beam direction $\hat{x}$ and the perpendicular axis $\hat{y}$ as the *longitudinal* ($M_\parallel$) and the *transverse* ($M_\perp$) magnetization, respectively. $M_\parallel$ was measured with a circular coil, coaxial with the centrifuge beam, whereas $M_\perp$ was quantified using a tilted coil (see caption to Fig. 1). The respective magnetizations were retrieved from the recorded EMF as

$$M_{\parallel(\perp)}(t) = n_c \mu_{\parallel(\perp)}(t) = -c_{\parallel(\perp)} \int_{-\infty}^{t} \mathcal{E}(t')dt', \quad (1)$$

with the coefficients $c_{\parallel(\perp)}$ calculated numerically for each coil [19]. To find the magnetic moment per molecule, $\mu_{\parallel(\perp)}$, we divided $M_{\parallel(\perp)}$ by the number density of centrifuged molecules $n_c = \eta P/k_B T$, where P and T are the gas pressure and temperature, k_B is the Boltzmann constant, and η is the fraction of molecules spun by the centrifuge. The intensity of our laser pulses ($\approx 10^{12}$ W/cm^2) is sufficient for adiabatically spinning the lowest rotational state only, dictating $\eta = 0.04$ at room temperature.

To apply an external magnetic field $\mathbf{B}$, two permanent magnets were introduced along the $\hat{z}$ axis (Fig. 1). Changing the gap between the magnets and their orientation, we were able to set the field strength at either 0.5 or 1 T, as well as flip its sign. Each wave form $\mathcal{E}(t)$ was averaged over 1,000 laser shots. Since the sign of the induced magnetization is defined by the direction of the molecular rotation, every experiment was repeated with the centrifuge rotation reversed, and the final signal $\mathcal{E}(t)$ was calculated as half the difference of the two measurements. Furthermore, the transverse magnetization $M_\perp$ must change its sign under the B-field inversion. Hence, it was determined from half the difference between the two EMF signals at two opposite directions of $\mathbf{B}$.

The observed longitudinal magnetization in the absence of the external magnetic field is shown in Fig. 2 for two values of the gas pressure. The detected EMF signals are on the scale of 100 μV (see inset) and correspond to the induced magnetic moment of up to $0.16\mu_B$/molecule. The clear shortening of both the rising time and the decay time of $\mu_\parallel(t)$ with increasing pressure suggests the collisional mechanism behind the induced magnetization. The spin-rotation (SR) coupling lifts the degeneracy of the three projections of oxygen's electronic spin $S(S_N = 0, \pm 1)$ on the angular momentum of the centrifuged molecules $\mathbf{N}$ [20]. If the collisional spin relaxation was much faster than the rotational one, the more energetically favorable state with $S_N = +1$ would acquire higher population than that with $S_N = -1$. This would generate a nonzero gas magnetization in the direction opposite to $\mathbf{N}$, in agreement with our observations.

On the other hand, the experimental absolute values of $M_\parallel$ are too high to be explained by this simple model.

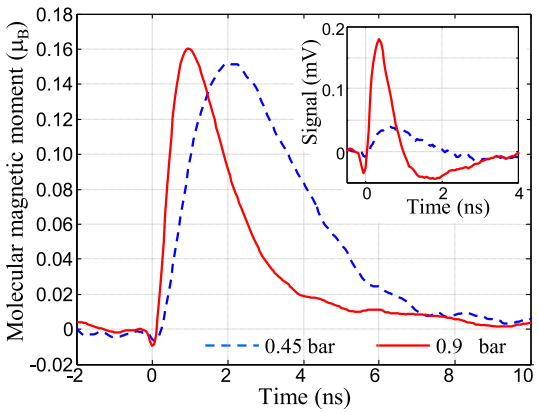

FIG. 2. Centrifuge-induced longitudinal magnetic moment $\mu_\parallel$ in oxygen gas without external magnetic field, in units of Bohr magneton μ_B. Inset shows raw EMF signals $\mathcal{E}(t)$ recorded under the pressure of 0.45 bar (dashed blue) and 0.9 bar (solid red). Time zero corresponds to the arrival of the centrifuge pulse, whose duration of $\approx$30 ps was adjusted for the excitation of O_2 molecules to the rotational level $N = 33$.

Indeed, the imbalance between the $S_N = \pm 1$ states *at constant* N is governed by the Boltzmann factor $\tanh(\Delta E_{N\pm1}/k_B T)$, with $\Delta E_{N\pm1}$ being the energy difference between the two states. For $N = 33$ at room temperature, this factor of only 0.3% would result in the magnetization of more than an order of magnitude smaller than the observed one. Because of the excellent agreement between the calculated and the detected transverse moment $\mu_\perp$ (see below), we conclude that the experimentally determined magnitude of $\mu_\parallel$ is correct. We therefore associate its large value with the fact that the relaxation time scales for the electronic spin and the molecular angular momentum are not separable [16,21]. Hence, the relaxation dynamics of the two spin components $S_N = \pm 1$, occurring *simultaneously with the decay of* N, may be quite different. For instance, the conservation of the total angular momentum $J = N - 1$ during the relaxation process $(N \to N - 2; S_N = -1 \to S_N = +1)$ could result in a higher spin flip rate from $S_N = -1$ to $S_N = +1$ than in the opposite direction, for which the analogous $\Delta J = 0$ relaxation channel is unavailable. A numerical estimate shows that a 50% difference in the respective decay constants of the two spin components would bring the transient longitudinal magnetization close to our experimental findings. However, the validity of this model is yet to be explored.

To study the induced magnetization further, we applied an external magnetic field along the vertical ($\hat{z}$) axis. In a recent study of oxygen superrotors in an external magnetic field [22–24], it was found that the spin-rotation coupling serves as an efficient mediator between the applied B-field and the molecular rotation, enabling magnetic control of the rotational degree of freedom. Here, we demonstrate the effect of SR coupling on the centrifuge-induced magnetization.

The green dotted line in Fig. 3 shows the effect of the applied field on the longitudinal magnetic moment. As expected, the latter undergoes Larmor precession, resulting in the oscillatory behavior of $\mu_\parallel(t)$. In comparison to the same signal at $B = 0$ (blue dashed line), the rising edge becomes steeper in the presence of the field. While in the field-free case the rise time is of the order of a few nanoseconds and depends on the gas pressure, it becomes shorter than 0.5 ns and no longer changes with pressure when $B \neq 0$. We attribute this behavior to the SR-mediated spin-flipping Raman transitions [25], which occur during the forced molecular rotation by the centrifuge (rather than during the postcentrifuge collisional thermalization) in the presence of the external B-field and create an imbalance between the $S_N = +1$ and $S_N = -1$ states. Understanding the details of this process will require further theoretical analysis.

Figure 3 shows the appearance of a strong magnetization in the transverse direction (red solid curve). It reaches $0.65\mu_B$ per every centrifuged molecule and creates a magnetic flux density $B_\perp = \mu_0 M_\perp$ of almost 40 mG in the gas under the pressure of a half atmosphere (here, μ_0 is

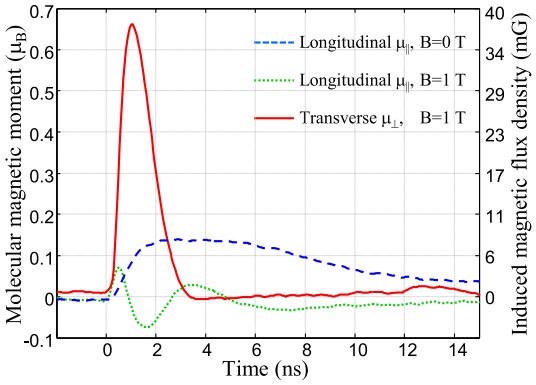

FIG. 3. Longitudinal (dotted green) and transverse (solid red) magnetic moments of O_2 molecules under the pressure of 0.5 bar, centrifuged to the rotational quantum number $N = 89$, in the external magnetic field of 1 T. Longitudinal moment in the absence of B-field is plotted for comparison (blue dashed). Note the much higher degree of rotational excitation than in Fig. 2 ($N = 33$), which explains the longer decay time. Right vertical axis shows the corresponding values of the induced magnetic flux density.

the vacuum permeability). Such a large value of $M_\perp$ can be understood by analyzing the rotational dynamics of paramagnetic superrotors in an external magnetic field [22,23]. An optical centrifuge drives the molecules to a state of high angular momentum $\mathbf{N}$, while an applied magnetic field generates a torque on the electronic spin $\mathbf{S}$. If the field is not strong enough to decouple the two vectors (for oxygen, of order of 1 T or below), SR interaction causes the angular momentum to precess together with $\mathbf{S}$. The precession frequency depends on the mutual orientation of $\mathbf{N}$ and $\mathbf{S}$ in the following way [23]:

$$\mathbf{\Omega}_{N,S_N}(B) = -\frac{\mu_B g S_N}{\hbar N}\mathbf{B} = -\Omega_N(B) S_N \hat{z}, \qquad (2)$$

where g is the electron g factor and $\hbar$ is the reduced Planck constant. It is evident from the above expression that the two spin components $S_N = \pm 1$ precess in opposite directions. The process is illustrated in Fig. 1 by the three disk-shaped distributions of molecular axes in a high-N superrotor state, corresponding to the three possible projections of the electronic spin on the molecular angular momentum. After a quarter precession period (or 0.8 ns for $B = 1$ T and $N = 89$), the total magnetic moment in the direction perpendicular to both the initial angular momentum and the applied magnetic field reaches its maximum value of $2/3\mu_B|g| \approx 1.3\mu_B$ per molecule, close to the observed moment in Fig. 3. The smaller magnitude of $\mu_\perp$ is in fact well anticipated due to the comparable time scales of the magnetic precession and rotational relaxation [16].

As expected, lowering the pressure decreased the magnitude of $\mu_\perp$ proportionally and also prolonged its lifetime, allowing us to observe a larger number of oscillations, as

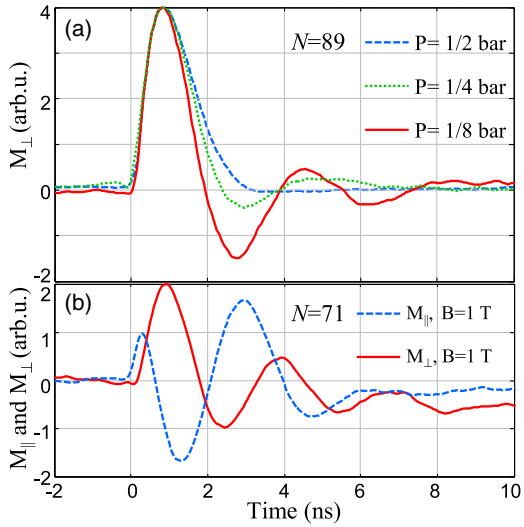

FIG. 4. (a) Dependence of the centrifuge-induced transverse magnetization on the pressure of oxygen gas in the external magnetic field of 1 T. Molecules have been excited to $N = 89$. To show the precession oscillations more clearly, all signals have been normalized to the same peak value at 0.8 ns. (b) Longitudinal (dashed blue) and transverse (solid red) magnetization of the gas of O_2 molecules centrifuged to the rotational quantum number of $N = 71$ in the external magnetic field of 1 T.

shown in Fig. 4(a). In contrast to the longitudinal signal, no change was detected in the growth rate of $\mu_\perp$ with pressure, which confirms its noncollisional nature. Identical precession frequencies and a $\pi/2$ phase shift between the oscillation of the longitudinal and transverse magnetic moments, visible in Fig. 4(b), further corroborates their suggested origins.

An apparent difference between the precession frequencies of the transverse magnetization in the upper and lower panels of Fig. 4 is due to the inverse proportionality of $\Omega_N(B)$ on the rotational quantum number N, described by Eq. (2). Figures 5(a)–(c) present a quantitative analysis of this dependence. Different values of the molecular angular momentum were obtained by controlling the terminal frequency of the centrifuge pulse by means of adjusting its duration [18]. Our experimental results (green, blue, and red dots for $N = 43$, 61, and 71, respectively) are well described by the theoretically expected functional form (solid lines):

$$\mathcal{E}(t) = -\frac{d}{dt} A_N (\sin \Omega_{N,+1} t + \sin \Omega_{N,-1} t) e^{-t/\tau_N}, \quad (3)$$

with the fitting parameters A_N and τ_N and the two terms in the brackets corresponding to the two counterrotating spin components $S_N = \pm 1$. Note that using $\Omega_{N,+1} = \Omega_{N,-1} \equiv \Omega_N = \mu_B g B/(\hbar N)$ in accordance with Eq. (2) did not produce satisfactory fits, owing to the partial decoupling of **S** from **N** at high values of the magnetic field [23]. To account for this effect, we numerically diagonalized the spin-rotational Hamiltonian in the presence of an external magnetic field:

$$\hat{H}_{SR} = \gamma \mathbf{NS} - \lambda \frac{(\mathbf{NS})^2}{N(N+1)} - g\mu_B \mathbf{SB}, \quad (4)$$

where γ and λ are the spin-rotational and the spin-spin interaction energies of oxygen, respectively [26]. The exact frequencies $\Omega_{N,\pm 1}$ were calculated from the spectrum of the above Hamiltonian for given values of N and B. The magnetization decay times τ_N, retrieved from the fit as 3.1 ± 0.6 ns for $N = 71$, 2.4 ± 0.4 ns for $N = 61$ and 1.8 ± 0.4 ns for $N = 43$, are in agreement with the previously found time constants for the collision-induced rotational decay [16]. Lowering the strength of the applied magnetic field to half its value, i.e. to $B = 0.5$ T, resulted in the anticipated decrease of the precession frequency, as can be seen by comparing plots (c) and (d) in Fig. 5.

To summarize, we have demonstrated experimentally the ability of an optical centrifuge to induce macroscopic magnetization in a gas of paramagnetic molecules under ambient conditions. Two mechanisms have been identified and studied. The magnetic moment in the direction of the laser beam was induced by the centrifuge field alone and seems to result from spin-flipping collisions. The surprisingly high magnitude of this longitudinal component requires further investigation.

The second type of magnetization was observed in the transverse direction perpendicular to the centrifuge beam. It requires an external magnetic field and is well understood in

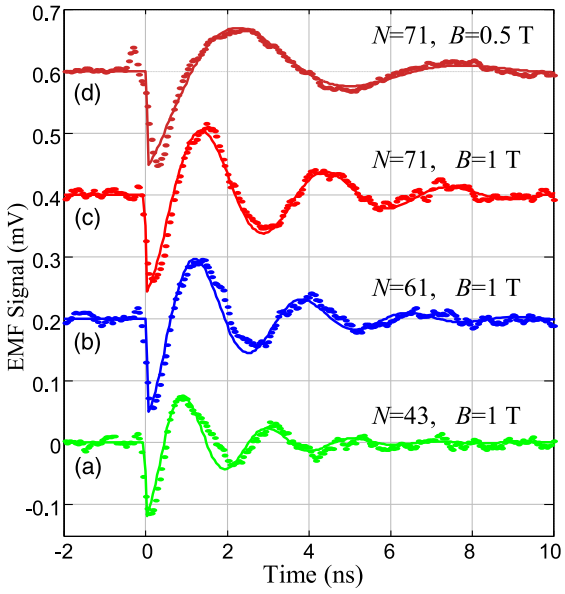

FIG. 5. (a)–(c) Experimentally detected (dots) and numerically calculated (solid lines) transverse EMF signal $\mathcal{E}(t)$ as a function of the rotational quantum number N in the external magnetic field of 1 T. For clarity, each consecutive plot has been shifted up by 0.2 mV. (d) Same as in (c), but with the magnetic field strength lowered to 0.5 T.

the framework of the spin-rotational dynamics of paramagnetic superrotors. Following the transfer of angular momentum from the centrifuge field to the molecular rotation, the evolution of the spin-rotational wave packet results in a transient polarization of the electronic spin. The latter process can be viewed as a rotational analogof the spin-orbital evolution, also known to produce transient electronic polarization in electronically excited atoms [10,11].

Polarization transfer from the molecular rotation to the nuclear spin has been discussed theoretically [27,28] and demonstrated experimentally [29] with low rotational excitation of HCl molecules by resonant laser pulses. Hence, extending the use of the nonresonant centrifuge-induced polarization of gases to their nuclear spins is an appealing prospect, especially in the context of NMR-based medical imaging.

We would like to thank Johannes Floß for many helpful discussions, and the electronics shop of the Department of Chemistry at UBC for invaluable continuous support. This research has been supported by the grants from Canada Foundation for Innovation (CFI), British Columbia Knowledge Development Fund (BCKDF), and Natural Sciences and Engineering Research Council of Canada (NSERC).

[1] T. G. Walker and W. Happer, Rev. Mod. Phys. **69**, 629 (1997).
[2] B. M. Goodson, J. Magn. Reson. **155**, 157 (2002).
[3] P. J. Keliher, F. B. Dunning, M. R. O'Neill, R. D. Rundel, and G. K. Walters, Phys. Rev. A **11**, 1271 (1975).
[4] L. G. Gray, K. W. Giberson, C. Cheng, R. S. Keiffer, F. B. Dunning, and G. K. Walters, Rev. Sci. Instrum. **54**, 271 (1983).
[5] C. Hernandez-Garcia, P. G. O'Shea, and M. L. Stutzman, Phys. Today **61**, No. 2, 44 (2008).
[6] T. J. Gay, in *Advances In Atomic, Molecular, and Optical Physics* (Academic Press, New York, 2009), Vol. 57, pp. 157–247.
[7] W. Happer and W. A. Van Wijngaarden, Hyperfine Interact. **38**, 435 (1987).
[8] P. Lambropoulos, Phys. Rev. Lett. **30**, 413 (1973).
[9] T. Nakajima and P. Lambropoulos, Europhys. Lett. **57**, 25 (2002).
[10] M. A. Bouchene, S. Zamith, and B. Girard, J. Phys. B **34**, 1497 (2001).
[11] T. Nakajima, Appl. Phys. Lett. **84**, 3786 (2004).
[12] B. Lancor, E. Babcock, R. Wyllie, and T. G. Walker, Phys. Rev. Lett. **105**, 083003 (2010).
[13] T. G. Walker, J. Phys. Conf. Ser. **294**, 012001 (2011).
[14] J. Karczmarek, J. Wright, P. Corkum, and M. Ivanov, Phys. Rev. Lett. **82**, 3420 (1999).
[15] D. M. Villeneuve, S. A. Aseyev, P. Dietrich, M. Spanner, M. Y. Ivanov, and P. B. Corkum, Phys. Rev. Lett. **85**, 542 (2000).
[16] A. A. Milner, A. Korobenko, and V. Milner, New J. Phys. **16**, 093038 (2014).
[17] O. Korech, U. Steinitz, R. J. Gordon, I. Sh. Averbukh, and Y. Prior, Nat. Photonics **7**, 711 (2013).
[18] A. Korobenko, A. A. Milner, and V. Milner, Phys. Rev. Lett. **112**, 113004 (2014).
[19] See Supplemental Material at http://link.aps.org/supplemental/10.1103/PhysRevLett.118.243201 for the details of our procedure to retrieve the absolute value of the induced magnetization.
[20] G. Herzberg, *Molecular Spectra and Molecular Structure*, 2nd ed. (Krieger Publishing Co, Malabar, FL, 1950), Vol. I.
[21] A. A. Milner, A. Korobenko, K. Rezaiezadeh, and V. Milner, Phys. Rev. X **5**, 031041 (2015).
[22] A. A. Milner, A. Korobenko, J. Floß, I. Sh. Averbukh, and V. Milner, Phys. Rev. Lett. **115**, 033005 (2015).
[23] J. Floß, J. Phys. B **48**, 164005 (2015).
[24] A. Korobenko and V. Milner, J. Phys. B **48**, 164004 (2015).
[25] M. Bérard, P. Lallemand, J. P. Cebe, and M. Giraud, J. Chem. Phys. **78**, 672 (1983).
[26] J. Brown and A. Carrington, *Rotational Spectroscopy of Diatomic Molecules* (Cambridge University Press, West Nyack, NY, 2003).
[27] T. P. Rakitzis, Phys. Rev. Lett. **94**, 083005 (2005).
[28] D. Sofikitis and T. P. Rakitzis, Phys. Rev. A **92**, 032507 (2015).
[29] D. Sofikitis, L. Rubio-Lago, M. R. Martin, D. J. A. Brown, N. C.-M. Bartlett, R. N. Zare, and T. P. Rakitzis, Phys. Rev. A **76**, 012503 (2007).